PROCEEDINGS OF SCIENCE

Observation of Large-Scale Anisotropy in Very-High-Energy Cosmic Ray Protons with LHAASO-KM2A

Jiayin He,[a,b,*] **Yi Zhang**[a,b] **and Qiang Yuan**[a,b]
on behalf of the LHAASO Collaboration
(a complete list of authors can be found at the end of the proceedings)

[a] *Key Laboratory of Dark Matter and Space Astronomy, Purple Mountain Observatory, Chinese Academy of Sciences, Nanjing 210023, China*

[b] *School of Astronomy and Space Science, University of Science and Technology of China, Hefei 230026, China*

E-mail: hejy@pmo.ac.cn, zhangyi@pmo.ac.cn, yuanq@pmo.ac.cn

We present a measurement of large-scale anisotropies in high-purity protons utilizing the Large High Altitude Air Shower Observatory (LHAASO). We analyzed data collected over three years from the kilometer-squared array (KM2A). Proton data was selected using a cut based on the ratio of muonic to electromagnetic components, akin to the gamma/background discrimination method used in KM2A. The proton sample achieved a purity of up to 80%, with reconstructed energies ranging from 10 TeV to 220 TeV. We conducted an analysis of the energy evolution of dipole anisotropy in protons within this energy range and identified that the turnover energy in amplitude and phase occurs at a lower energy compared to samples of heavier nuclei.

39th International Cosmic Ray Conference (ICRC2025)
15–24 July 2025
Geneva, Switzerland

ICRC 2025
The Astroparticle Physics Conference
Geneva July 15-24, 2025

*Speaker

PoS(ICRC2025)286

1. Introduction

Cosmic ray large-scale anisotropy manifests as a dipole-dominated structure, with energy-dependent amplitude and phase observed by multiple ground-based experiments. For all-particle cosmic rays, the dipole amplitude ranges from 10^{-4} to 10^{-3} between TeV and 10 PeV energies [1–6]. Its evolution shows: amplitude increases from TeV to 10 TeV, decreases from 10 TeV to 100 TeV, reaches a minimum around 100 TeV, then increases again. The phase remains stable at 20°–50° from TeV to tens of TeV but reverses direction above ~100 TeV, stabilizing near 100°.

Cosmic rays comprise protons, helium, and other heavier nuclei. Although protons dominate the TeV flux, their large-scale anisotropy remain unmeasured. Space experiments like Fermi-LAT lack sufficient statistics due to small effective areas and low fluxes. Fermi-LAT's 8-year analysis found proton dipole amplitudes consistent with background fluctuations [7]. Ground arrays have large areas but cannot isolate proton components, rendering proton anisotropy measurements unavailable. The LHAASO-KM2A, equipped with electromagnetic detectors (EDs) and muon detectors (MDs), has the capacity to distinguish γ-rays and cosmic ray backgrounds, which makes it the most sensitive detector above 25 TeV among the ground-based experiments [8]. In this study, with the data from KM2A, we select a sample of high-purity cosmic-ray protons, enabling us to precisely measure the pure proton anisotropy.

2. LHAASO Experiment

The LHAASO experiment, located at Haizi Mountain in Daocheng, Sichuan province, China (100.01°E, 29.35°N), is a hybrid ground-based experiment designed to take advantage of its wide field of view, large detected area, and high duty cycles[9]. The LHAASO experiment consists of three sub-arrays: KM2A, an array with an area of 1.3 square kilometers; WCDA, water Cherenkov detector arrays spanning 78000 m^2; and WFCTA, wide field of view Cherenkov/fluorescence telescopes. The full array of KM2A comprises 5195 EDs and 1188 MDs, and has been running since July 20, 2021.

3. Data Analysis

In our analysis, the data from the KM2A full array is used, accumulated in the period from July 20, 2021, to July 19, 2024. To ensure the high quality of data, some cut conditions are applied for selection: the number of triggered electromagnetic detectors (EDs) after applying the noise filter was at least 20; the reconstructed shower core was situated within the array, and the zenith angle was less than 40°.

To isolate a high-purity proton dataset, we leverage information from underground muon detectors using Monte Carlo data. The muon content in atmospheric showers highly correlates with the primary particle's mass composition. When primary cosmic rays interact in the atmosphere, they induce extensive air showers containing secondary electromagnetic components and muons. Crucially, hadronic showers produce significantly more muons than electromagnetic showers from gamma rays. This property enables gamma/hadron separation through muon-to-EM ratios, and a technique combining the electromagnetic particles and muons has been employed in KM2A gamma-ray analyses [8].

The parameter applied for gamma/background discrimination is defined as

$$R = \log\frac{N_\mu + 10^{-4}}{N_e}, \tag{1}$$

where N_μ and N_e are the number of muons and electromagnetic particles, respectively. And 10^{-4} is used for the cases with null muons. Indeed, the same methodology can be employed to distinguish protons from heavy nuclei, as heavy nuclei produce substantially more muons during atmospheric shower development. Figure 1 shows how we select proton events from cosmic rays. The cosmic ray sample comprises events from both protons and heavier nuclei than protons, and their distributions of R are shown in the left plot, and the γ-like events are excluded in our analysis, i.e., the target sample with a R interval $(-2, R^\star)$, where $R^\star$ is determined by the purity of proton, which is shown in the right plot. In this work, the purity is set to be 80%, resulting in the cut indicated as the vertical dashed line about -0.87. Subsequently, we find the criteria satisfying 80% proton purity in other energy bins. When this procedure is done, the energy is calibrated using ρ_{50} estimator, which is based on the lateral distribution of the electromagnetic component of the shower [8]. In this study, we employed the same technique to obtain a proton-plus-helium sample with 90% purity, which, with the sample of all particles, serves as the reference sample for our measurements. The energy estimator for the sample of proton-plus-helium and the sample of all particles is similar to the work of [10, 11].

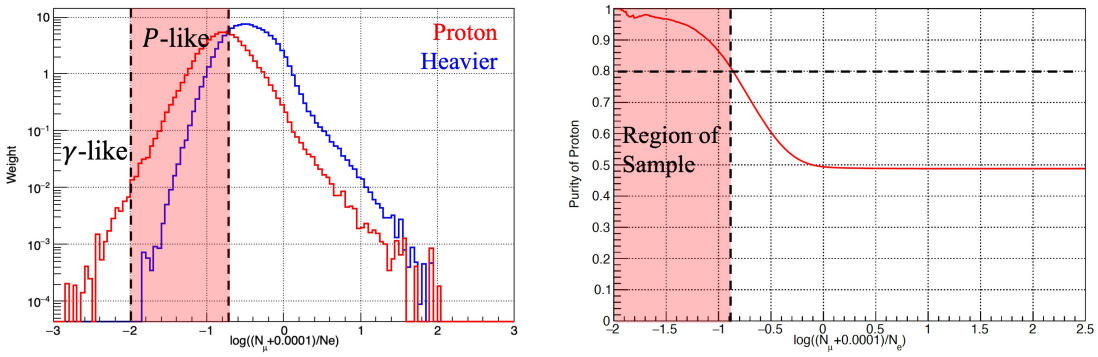

Figure 1: Selection of proton-like events (left) and the proton purity in a proton-like sample (right). In this example, the cosmic ray has reconstructed energy $\log(E_{rec}/\mathrm{TeV}) \in [1.4, 1.6)$.

To estimate the isotropic background, we perform an iterative method based on the zenith angle method, i.e., equi-zenith angle method [12, 13]. The relative intensity is computed by minimizing the chi-square

$$\chi^2 = \sum_{i,j,k} \frac{\frac{N(\theta_i,\phi_j,\tau_k)}{I(\alpha_\rho,\delta_\nu)} - \frac{1}{n_{\theta_i}-1}\sum_{j'\neq j}\frac{N(\theta_i,\phi_{j'},\tau_k)}{I(\alpha_{\rho'},\delta_{\nu'})}}{\sigma^2_{i,j,k}}, \tag{2}$$

where the relative intensity is defined by the ratio of observed events N over isotropic backgrounds B, i.e., $I(\alpha,\delta) = N(\alpha,\delta)/B(\alpha,\delta)$. The number of events in the arrival direction of zenith θ_i, azimuth ϕ_j in local horizontal coordinates given a time interval τ_k is $N(\theta_i,\phi_j,\tau_k)$, and this direction points to equinoctial coordinates (α_ρ,δ_ν). And n_{θ_i} and $\sigma_{i,j,k}$ are the number of windows in the i-th zenith ring and the uncertainty of the numerator.

4. Results

The sky maps of relative intensity and significance are presented in Figure 2, which are smooth with a 30° radius top-hat function. The significance of two-dimensional maps is well beyond $5\,\sigma$, and the morphologies of the anisotropies evolve with energy with a significant change at about 60 TeV, both the value of the relative intensity and the positions of regions of hot/cold spots. A more straightforward way is to show the amplitude and phase of a dipole evolution with energies, which is obtained by fitting to the relative intensity projected on right ascension. Here, a harmonic function up to the 2nd order is employed, i.e.,

$$I(\alpha) = 1 + \sum_{i=1}^{2} A_i \cos(i(\alpha - \varphi_i)), \tag{3}$$

where A_i and φ_i are the amplitude and phase for dipole ($i = 1$)/quadrupole ($i = 2$).

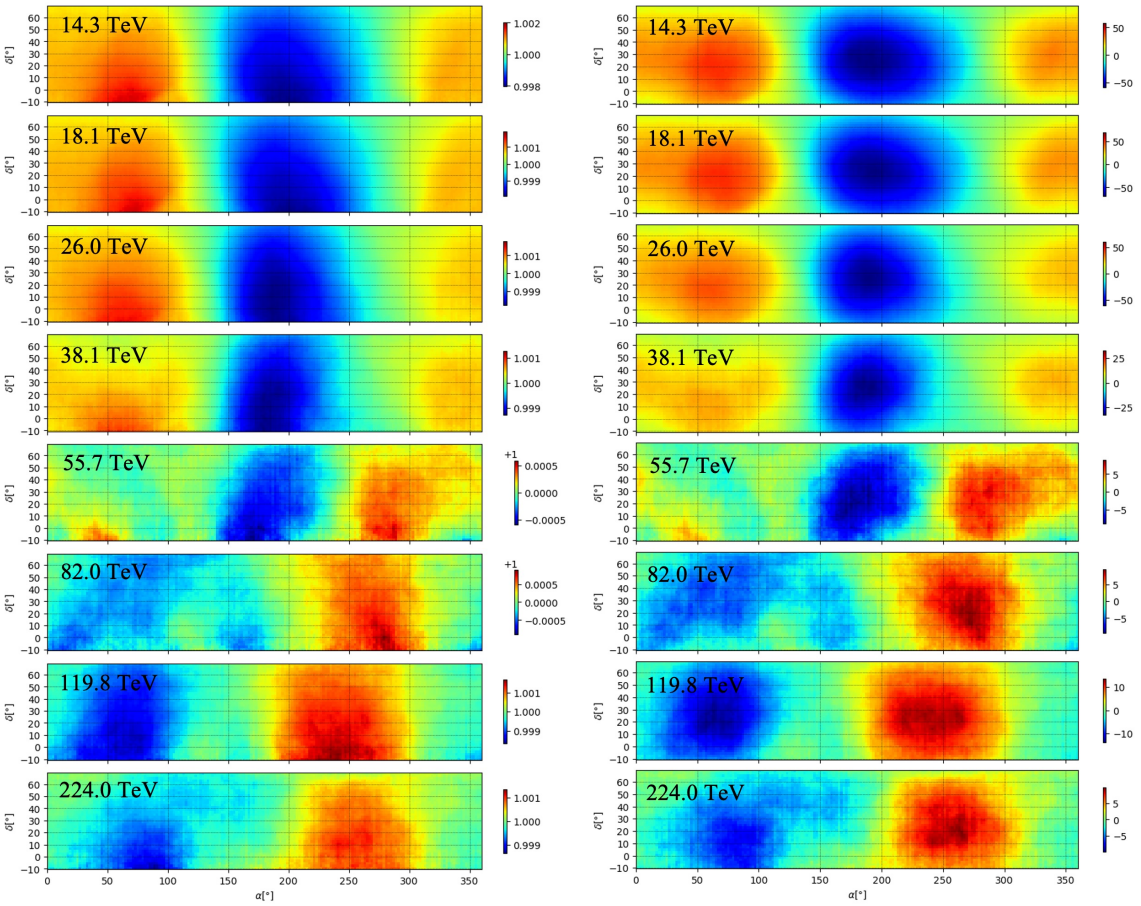

Figure 2: Sky maps of relative intensity (left) and significance (right) for proton-like samples. The maps have been smoothed with a 30° radius top-hat function.

The results are shown in Figure 3, where we also compare with the results of samples of proton-plus-helium and samples of all particles. From the plots we find that the turnover energies

for these samples: ~56 TeV for proton-like, ~70 TeV for proton-plus-helium, and ~130 TeV for all particles.

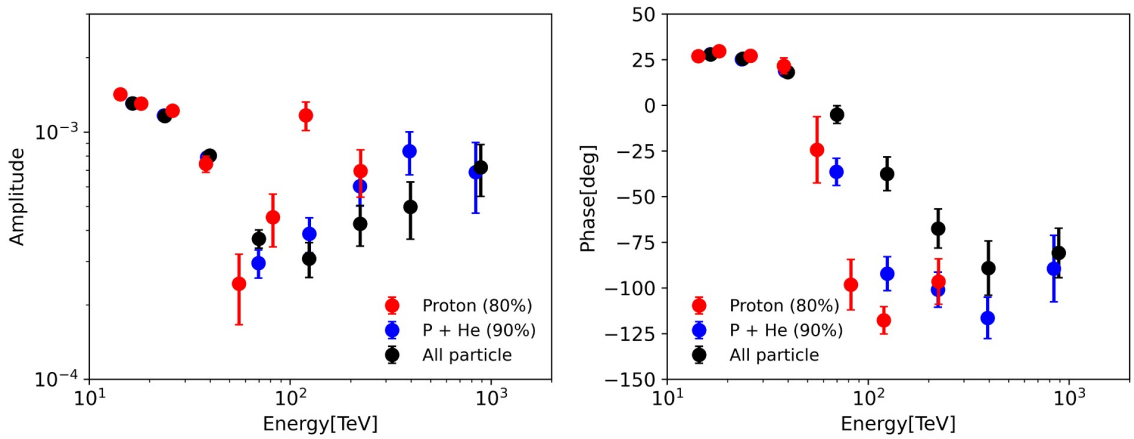

Figure 3: The evolutions of amplitude (left) and phase (right) of a dipole with energies.

Our measurement results impose significant constraints on existing theoretical models. The model involves local source and slow diffusion aimed to describe the coevolution of cosmic ray spectra and anisotropies, predicts the anisotropy of protons under charge-dependent (Z-dependent) and mass-dependent (A-dependent) scenarios [14]. We compare the measurements with the model expectations in Figure 4, neither the Z-dependent nor A-dependent predictions for proton anisotropy amplitude and phase evolution agree well with our experimental measurements. These measurements would severely restrict the parameter space of current models.

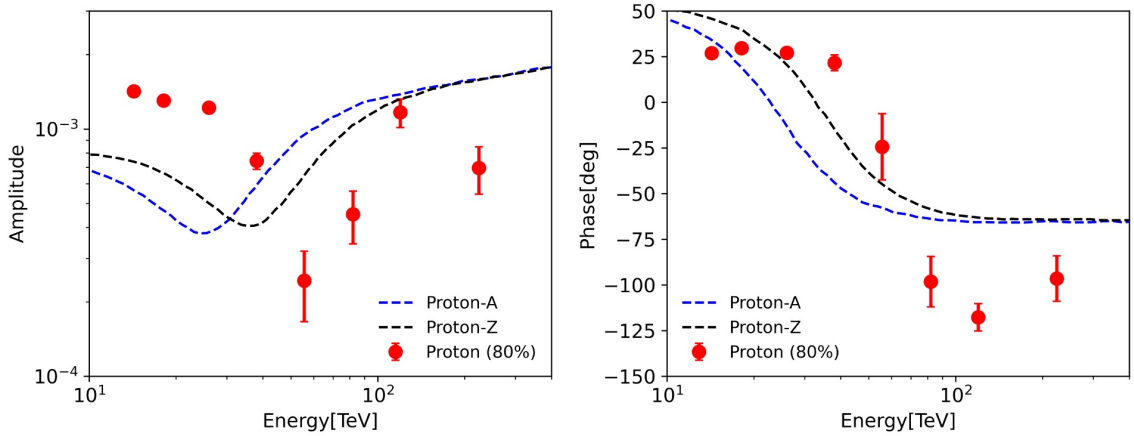

Figure 4: The measurements of the dipole of proton-like sample compared with the existing models [14].

5. Conclusion

This study presents a search for large-scale anisotropies with a sample of 80% proton purity above 10 TeV. The analysis utilizes KM2A full array data spanning from July 20, 2021, to July 19,

2024. A notable observation is a noticeable change in the anisotropy of protons around 60 TeV, and this change in the proton sample's anisotropy occurs earlier compared to the energy evolution of the large-scale anisotropy of all-particle cosmic rays and a high-purity sample of proton plus helium. Additionally, this research would exert a profound influence on the models and deepen the understanding of the propagation of cosmic rays in the Galaxy.

6. Acknowledgement

We would like to thank all staff members who work at the LHAASO site above 4400 meters above sea level year-round to maintain the detector and keep the water recycling system, electricity power supply, and other components of the experiment operating smoothly. We are grateful to the Chengdu Management Committee of Tianfu New Area for the constant financial support for research with LHAASO data. This research work is also supported by the National Natural Science Foundation of China (Nos. 12273114), the Project for Young Scientists in Basic Research of Chinese Academy of Sciences (No. YSBR-061) and the Program for Innovative Talents and Entrepreneur in Jiangsu.

References

[1] M. Amenomori et al. (The Tibet ASγ Collaboration), Science **314**, 439 (2006), URL https://doi.org/10.1126/SCIENCE.1131702.

[2] A. A. Abdo et al. (The Milagro Collaboration), The Astrophysical Journal **698**, 2121 (2009), URL https://dx.doi.org/10.1088/0004-637X/698/2/2121.

[3] B. Bartoli et al. (The ARGO-YBJ Collaboration), The Astrophysical Journal **861**, 93 (2018), URL https://dx.doi.org/10.3847/1538-4357/aac6cc.

[4] A. U. Abeysekara et al. (The HAWC Collaboration), The Astrophysical Journal **865**, 57 (2018), URL https://dx.doi.org/10.3847/1538-4357/aad90c.

[5] R. Abbasi et al. (The IceCube Collaboration), The Astrophysical Journal **746**, 33 (2012), URL https://dx.doi.org/10.1088/0004-637X/746/1/33.

[6] M. G. Aartsen et al. (The IceCube Collaboration), The Astrophysical Journal **765**, 55 (2013), URL https://dx.doi.org/10.1088/0004-637X/765/1/55.

[7] M. Ajello, L. Baldini, G. Barbiellini, D. Bastieri, K. Bechtol, R. Bellazzini, E. Bissaldi, R. D. Blandford, R. Bonino, E. Bottacini, et al., The Astrophysical Journal **883**, 33 (2019), URL https://dx.doi.org/10.3847/1538-4357/ab3a2e.

[8] F. Aharonian, Q. An, Axikegu, L. X. Bai, Y. X. Bai, Y. W. Bao, D. Bastieri, X. J. Bi, Y. J. Bi, H. Cai, et al., Chinese Physics C **45**, 025002 (2021).

[9] H. He and F. Collaboration, Radiation Detection Technology and Methods p. 002 (2018).

[10] H. Zhang, H. He, and C. Feng, Phys. Rev. D **106**, 123028 (2022), URL https://link.aps.org/doi/10.1103/PhysRevD.106.123028.

[11] Z. Cao et al. (The LHAASO Collaboration), Phys. Rev. Lett. **132**, 131002 (2024), URL https://link.aps.org/doi/10.1103/PhysRevLett.132.131002.

[12] M. Amenomori, S. Ayabe, D. Chen, S. W. Cui, Danzengluobu, L. K. Ding, X. H. Ding, C. F. Feng, Z. Y. Feng, X. Y. Gao, et al., ApJ **633**, 1005 (2005), number: 2.

[13] M. Amenomori, S. Ayabe, X. J. Bi, D. Chen, S. W. Cui, Danzengluobu, L. K. Ding, X. H. Ding, C. F. Feng, Z. Feng, et al., Science **314**, 439 (2006), number: 5798.

[14] B.-Q. Qiao, W. Liu, Y.-Q. Guo, and Q. Yuan, Journal of Cosmology and Astroparticle Physics **2019**, 007 (2019).

Full Authors List: LHAASO Collaboration

Zhen Cao[1,2,3], F. Aharonian[3,4,5,6], Y.X. Bai[1,3], Y.W. Bao[7], D. Bastieri[8], X.J. Bi[1,2,3], Y.J. Bi[1,3], W. Bian[7], A.V. Bukevich[9], C.M. Cai[10], W.Y. Cao[4], Zhe Cao[11,4], J. Chang[12], J.F. Chang[1,3,11], A.M. Chen[7], E.S. Chen[1,3], G.H. Chen[8], H.X. Chen[13], Liang Chen[14], Long Chen[10], M.J. Chen[1,3], M.L. Chen[1,3,11], Q.H. Chen[10], S. Chen[15], S.H. Chen[1,2,3], S.Z. Chen[1,3], T.L. Chen[16], X.B. Chen[17], X.J. Chen[10], Y. Chen[17], N. Cheng[1,3], Y.D. Cheng[1,2,3], M.C. Chu[18], M.Y. Cui[12], S.W. Cui[19], X.H. Cui[20], Y.D. Cui[21], B.Z. Dai[15], H.L. Dai[1,3,11], Z.G. Dai[4], Danzengluobu[16], Y.X. Diao[10], X.Q. Dong[1,2,3], K.K. Duan[12], J.H. Fan[8], Y.Z. Fan[12], J. Fang[15], J.H. Fang[13], K. Fang[1,3], C.F. Feng[22], H. Feng[1], L. Feng[12], S.H. Feng[1,3], X.T. Feng[22], Y. Feng[13], Y.L. Feng[16], S. Gabici[23], B. Gao[1,3], C.D. Gao[22], Q. Gao[16], W. Gao[1,3], W.K. Gao[1,2,3], M.M. Ge[15], T.T. Ge[21], L.S. Geng[1,3], G. Giacinti[7], G.H. Gong[24], Q.B. Gou[1,3], M.H. Gu[1,3,11], F.L. Guo[14], J. Guo[24], X.L. Guo[10], Y.Q. Guo[1,3], Y.Y. Guo[12], Y.A. Han[25], O.A. Hannuksela[18], M. Hasan[1,2,3], H.H. He[1,2,3], H.N. He[12], J.Y. He[12], X.Y. He[12], Y. He[10], S. Hernández-Cadena[7], B.W. Hou[1,2,3], C. Hou[1,3], X. Hou[26], H.B. Hu[1,2,3], S.C. Hu[1,3,27], C. Huang[17], D.H. Huang[10], J.J. Huang[1,2,3], T.Q. Huang[1,3], W.J. Huang[21], X.T. Huang[22], X.Y. Huang[12], Y. Huang[1,3,27], Y.Y. Huang[17], X.L. Ji[1,3,11], H.Y. Jia[10], K. Jia[22], H.B. Jiang[1,3], K. Jiang[11,4], X.W. Jiang[1,3], Z.J. Jiang[15], M. Jin[10], S. Kaci[7], M.M. Kang[28], I. Karpikov[9], D. Khangulyan[1,3], D. Kuleshov[9], K. Kurinov[9], B.B. Li[19], Cheng Li[11,4], Cong Li[1,3], D. Li[1,2,3], F. Li[1,3,11], H.B. Li[1,2,3], H.C. Li[1,3], Jian Li[4], Jie Li[1,3,11], K. Li[1,3], L. Li[29], R.L. Li[12], S.D. Li[14,2], T.Y. Li[7], W.L. Li[7], X.R. Li[1,3], Xin Li[11,4], Y. Li[7], Y.Z. Li[1,2,3], Zhe Li[1,3], Zhuo Li[30], E.W. Liang[31], Y.F. Liang[31], S.J. Lin[21], B. Liu[12], C. Liu[1,3], D. Liu[22], D.B. Liu[7], H. Liu[10], H.D. Liu[25], J. Liu[1,3], J.L. Liu[1,3], J.R. Liu[10], M.Y. Liu[16], R.Y. Liu[17], S.M. Liu[10], W. Liu[1,3], X. Liu[10], Y. Liu[8], Y. Liu[10], Y.N. Liu[24], Y.Q. Lou[24], Q. Luo[21], Y. Luo[7], H.K. Lv[1,3], B.Q. Ma[25,30], L.L. Ma[1,3], X.H. Ma[1,3], J.R. Mao[26], Z. Min[1,3], W. Mitthumsiri[32], G.B. Mou[33], H.J. Mu[25], A. Neronov[23], K.C.Y. Ng[18], M.Y. Ni[12], L. Nie[10], L.J. Ou[8], P. Pattarakijwanich[32], Z.Y. Pei[8], J.C. Qi[1,2,3], M.Y. Qi[1,3], J.J. Qin[4], A. Raza[1,2,3], C.Y. Ren[12], D. Ruffolo[32], A. Sáiz[32], D. Semikoz[23], L. Shao[19], O. Shchegolev[9,34], Y.Z. Shen[17], X.D. Sheng[1,3], Z.D. Shi[4], F.W. Shu[29], H.C. Song[30], Yu.V. Stenkin[9,34], V. Stepanov[9], Y. Su[12], D.X. Sun[4,12], H. Sun[22], Q.N. Sun[1,3], X.N. Sun[31], Z.B. Sun[35], N.H. Tabasam[22], J. Takata[36], P.H.T. Tam[21], H.B. Tan[17], Q.W. Tang[29], R. Tang[7], Z.B. Tang[11,4], W.W. Tian[2,20], C.N. Tong[17], L.H. Wan[21], C. Wang[35], G.W. Wang[4], H.G. Wang[8], J.C. Wang[26], K. Wang[30], Kai Wang[17], Kai Wang[36], L.P. Wang[1,2,3], L.Y. Wang[1,3], L.Y. Wang[19], R. Wang[22], W. Wang[21], X.G. Wang[31], X.J. Wang[10], X.Y. Wang[17], Y. Wang[10], Y.D. Wang[1,3], Z.H. Wang[28], Z.X. Wang[15], Zheng Wang[1,3,11], D.M. Wei[12], J.J. Wei[12], Y.J. Wei[1,2,3], T. Wen[1,3], S.S. Weng[33], C.Y. Wu[1,3], H.R. Wu[1,3], Q.W. Wu[36], S. Wu[1,3], X.F. Wu[12], Y.S. Wu[4], S.Q. Xi[1,3], J. Xia[4,12], J.J. Xia[10], G.M. Xiang[14,2], D.X. Xiao[19], G. Xiao[1,3], Y.L. Xin[10], Y. Xing[14], D.R. Xiong[26], Z. Xiong[1,2,3], D.L. Xu[7], R.F. Xu[1,2,3], R.X. Xu[30], W.L. Xu[28], L. Xue[22], D.H. Yan[15], T. Yan[1,3], C.W. Yang[28], C.Y. Yang[26], F.F. Yang[1,3,11], L.L. Yang[21], M.J. Yang[1,3], R.Z. Yang[4], W.X. Yang[8], Z.H. Yang[7], Z.G. Yao[1,3], X.A. Ye[12], L.Q. Yin[1,3], N. Yin[22], X.H. You[1,3], Z.Y. You[1,3], Q. Yuan[12], H. Yue[1,2,3], H.D. Zeng[12], T.X. Zeng[1,3,11], W. Zeng[15], X.T. Zeng[21], M. Zha[1,3], B.B. Zhang[17], B.T. Zhang[1,3], C. Zhang[17], F. Zhang[10], H. Zhang[7], H.M. Zhang[31], H.Y. Zhang[15], J.L. Zhang[20], Li Zhang[15], P.F. Zhang[15], P.P. Zhang[4,12], R. Zhang[12], S.R. Zhang[19], S.S. Zhang[1,3], W.Y. Zhang[19], X. Zhang[33], X.P. Zhang[1,3], Yi Zhang[1,12], Yong Zhang[1,3], Z.P. Zhang[4], J. Zhao[1,3], L. Zhao[11,4], L.Z. Zhao[19], S.P. Zhao[12], X.H. Zhao[26], Z.H. Zhao[4], F. Zheng[35], W.J. Zhong[17], B. Zhou[1,3], H. Zhou[7], J.N. Zhou[14], M. Zhou[29], P. Zhou[17], R. Zhou[28], X.X. Zhou[1,2,3], X.X. Zhou[10], B.Y. Zhu[4,12], C.G. Zhu[22], F.R. Zhu[10], H. Zhu[20], K.J. Zhu[1,2,3,11], Y.C. Zou[36], X. Zuo[1,3], (The LHAASO Collaboration)

[1] Key Laboratory of Particle Astrophysics & Experimental Physics Division & Computing Center, Institute of High Energy Physics, Chinese Academy of Sciences, 100049 Beijing, China
[2] University of Chinese Academy of Sciences, 100049 Beijing, China
[3] TIANFU Cosmic Ray Research Center, Chengdu, Sichuan, China
[4] University of Science and Technology of China, 230026 Hefei, Anhui, China
[5] Yerevan State University, 1 Alek Manukyan Street, Yerevan 0025, Armenia
[6] Max-Planck-Institut for Nuclear Physics, P.O. Box 103980, 69029 Heidelberg, Germany
[7] Tsung-Dao Lee Institute & School of Physics and Astronomy, Shanghai Jiao Tong University, 200240 Shanghai, China
[8] Center for Astrophysics, Guangzhou University, 510006 Guangzhou, Guangdong, China
[9] Institute for Nuclear Research of Russian Academy of Sciences, 117312 Moscow, Russia
[10] School of Physical Science and Technology & School of Information Science and Technology, Southwest Jiaotong University, 610031 Chengdu, Sichuan, China
[11] State Key Laboratory of Particle Detection and Electronics, China
[12] Key Laboratory of Dark Matter and Space Astronomy & Key Laboratory of Radio Astronomy, Purple Mountain Observatory, Chinese Academy of Sciences, 210023 Nanjing, Jiangsu, China
[13] Research Center for Astronomical Computing, Zhejiang Laboratory, 311121 Hangzhou, Zhejiang, China
[14] Shanghai Astronomical Observatory, Chinese Academy of Sciences, 200030 Shanghai, China
[15] School of Physics and Astronomy, Yunnan University, 650091 Kunming, Yunnan, China
[16] Key Laboratory of Cosmic Rays (Tibet University), Ministry of Education, 850000 Lhasa, Tibet, China
[17] School of Astronomy and Space Science, Nanjing University, 210023 Nanjing, Jiangsu, China
[18] Department of Physics, The Chinese University of Hong Kong, Shatin, New Territories, Hong Kong, China
[19] Hebei Normal University, 050024 Shijiazhuang, Hebei, China
[20] Key Laboratory of Radio Astronomy and Technology, National Astronomical Observatories, Chinese Academy of Sciences, 100101 Beijing, China
[21] School of Physics and Astronomy (Zhuhai) & School of Physics (Guangzhou) & Sino-French Institute of Nuclear Engineering and Technology (Zhuhai), Sun Yat-sen University, 519000 Zhuhai & 510275 Guangzhou, Guangdong, China
[22] Institute of Frontier and Interdisciplinary Science, Shandong University, 266237 Qingdao, Shandong, China

PoS(ICRC2025)286

[23] APC, Université Paris Cité, CNRS/IN2P3, CEA/IRFU, Observatoire de Paris, 119 75205 Paris, France
[24] Department of Engineering Physics & Department of Physics & Department of Astronomy, Tsinghua University, 100084 Beijing, China
[25] School of Physics and Microelectronics, Zhengzhou University, 450001 Zhengzhou, Henan, China
[26] Yunnan Observatories, Chinese Academy of Sciences, 650216 Kunming, Yunnan, China
[27] China Center of Advanced Science and Technology, Beijing 100190, China
[28] College of Physics, Sichuan University, 610065 Chengdu, Sichuan, China
[29] Center for Relativistic Astrophysics and High Energy Physics, School of Physics and Materials Science & Institute of Space Science and Technology, Nanchang University, 330031 Nanchang, Jiangxi, China
[30] School of Physics & Kavli Institute for Astronomy and Astrophysics, Peking University, 100871 Beijing, China
[31] Guangxi Key Laboratory for Relativistic Astrophysics, School of Physical Science and Technology, Guangxi University, 530004 Nanning, Guangxi, China
[32] Department of Physics, Faculty of Science, Mahidol University, Bangkok 10400, Thailand
[33] School of Physics and Technology, Nanjing Normal University, 210023 Nanjing, Jiangsu, China
[34] Moscow Institute of Physics and Technology, 141700 Moscow, Russia
[35] National Space Science Center, Chinese Academy of Sciences, 100190 Beijing, China
[36] School of Physics, Huazhong University of Science and Technology, Wuhan 430074, Hubei, China

PoS(ICRC2025)286